

P_T -imbalance in dimuon+jet production as a signal of partonic energy loss in heavy ion collisions at LHC

I.P. Lokhtin, A.V. Sherstnev, and A.M. Snigirev,

M.V. Lomonosov Moscow State University, D.V. Skobeltsyn Institute of Nuclear Physics
119992, Vorobievsky Gory, Moscow, Russia

E-mail: igor@lav01.sinp.msu.ru

Abstract

We consider a hard jet production tagged by a muon pair in ultrarelativistic heavy ion collisions. The process cross section is calculated by the ComPHEP Monte-Carlo generator taking into account full γZ interference pattern at LHC energies. We have found that reasonable statistics, 1000 events per 1 month of LHC run with lead beams, can be expected for realistic geometrical acceptance and kinematic cuts. The transverse momentum imbalance due to interactions of jet partons in the medium is evaluated for $\mu^+\mu^-$ pair+jet correlation, as well as for the correlation between $\mu^+\mu^-$ pair and a leading particle in a jet. Theoretical and experimental uncertainties of these observables are discussed.

PACS: 12.38Mh, 24.85.+p, 25.75.+r

Keywords: jet quenching, partonic energy loss, dileptons, relativistic nuclear collisions

1 Introduction

One of the important tools to study properties of quark-gluon plasma (QGP) in ultrarelativistic heavy ion collisions is a QCD jet production. Medium-induced energy loss of energetic partons, the so-called jet quenching, has been proposed to be very different in cold nuclear matter and in QGP, resulting in many challenging observable phenomena [1]. Recent RHIC data on suppression of inclusive high- p_T charge and neutral hadron production from STAR [2], PHENIX [3], PHOBOS [4] and BRAHMS [5] are in agreement with the jet quenching hypothesis [6]. However direct event-by-event reconstruction of jets and their characteristics is not available in RHIC experiments at the moment, while the assumption that integrated yield of all high- p_T particles originates only from jet fragmentation is not obvious.

At LHC a new regime of heavy ion physics will be reached at $\sqrt{s_{NN}} = 5.5$ TeV where hard and semi-hard QCD multiparticle production can dominate over underlying soft events. The initial gluon densities in Pb-Pb reactions at LHC are expected to be significantly higher than at RHIC, implying stronger partonic energy loss which can be observable in various new channels [7, 8, 9]. In particular, the potentially important process is production of a single jet opposite to a gauge boson in $\gamma + \text{jet}$ [10] and $Z + \text{jet}$ [11] or a virtual photon in $(\gamma^* \rightarrow l\bar{l}) + \text{jet}$ [12] final states, dominantly through processes such as

$$qg \rightarrow q + \text{jet}; \quad qg \rightarrow qZ; \quad qg \rightarrow q + \text{jet} :$$

In heavy ion collisions, the relative p_T between the jet (or leading particle in a jet) and the boson becomes imbalanced due to interactions of the jet partons in the medium.

In the $\gamma + \text{jet}$ case the main problem arises from the jet pair production background when a leading γ in the jet is misidentified as a photon. The "photon isolation" criteria usually used in pp collisions do not work with the same efficiency in high multiplicity heavy ion interactions [13]. Thus, the question of adequate using photon+jet correlation to study jet quenching requires further investigation. On the other hand, the production of jet tagged by dileptons is not affected significantly by backgrounds and can be used to observe p_T -imbalance as a signal of medium-induced partonic energy loss.

In this Letter we analyze dimuon+jet production (including both $\gamma \rightarrow Z \rightarrow l\bar{l} + \text{jet}$ modes) in heavy ion collisions at the LHC. In Sect. 2 the cross section of this process is calculated by ComPHEP Monte-Carlo generator and the expected event rate is estimated for realistic geometrical acceptance and kinematic cuts. Sect. 3 describes shortly the model of partonic energy loss in QGP used to calculate p_T -imbalance between $l\bar{l}$ pair and jet (or leading particle in a jet). Discussion on numerical results and their experimental and theoretical uncertainties can be found in Sect. 4, summary – in Sect. 5.

2 Dilepton+ jet production at LHC

We use the ComPHEP Monte-Carlo generator [14] for cross section calculation of dilepton+ jet process and subsequent generation of event for this process. ComPHEP is a general, tree level generator, which allows one to study almost all processes $2 \rightarrow N$ (up to $N = 5$) in the framework of the usual technique of Feynman diagrams squared for different models (SM, MSSM, many other...). It generates, squares and symbolically calculates a set of Feynman diagrams for a given process and creates a numeric Monte-Carlo generator for the process. This MC generator allows one to compute cross sections (with applied cuts), to build distributions and to generate events with partons in the final state; the initial partons are convoluted with parton distribution functions (PDF).

For simplification of our calculation and event generation we apply a special hash-model in ComPHEP [15]. In this model a unitary rotation of down quarks transfers Cabibbo-Kobayashi-Maskawa (CKM) matrix elements from interaction vertices to parton distribution functions. It allows one to unify two light quark generations to one only. As a result, this trick reduces significantly number of subprocesses which we need to take into account for the process. This model applies two approximations:

u (u, c) and d_h (d, s) quarks are massless;

b and t quarks do not interact with light quarks and CKM matrix element $V_{cb} = 1$.

In the problem of dilepton+ jet investigation the influence of factors violating these conditions is very small so we can soundly use this approximation.

There are nine subprocesses contributed to the process of the dilepton+ jet production in the framework of SM with hash-approximation. Feynman diagrams for the subprocesses are depicted on fig.1. We use the following physics parameter values: $\alpha_s = 0.1279$, $\sin^2 \theta_w = 0.2311$, $M_Z = 91.1876$ GeV, $M_{Z'} = 2.4368$ GeV, $M_{\gamma} = 105.7$ MeV, $M_b = 4.35$ GeV, PDF are taken from ctEq51 [16]. We apply a following set of "loose" cuts for event generation. In the further investigation these cuts have been strengthened:

$p_T > 5$ GeV/c and $p_T^{\text{jet}} > 20$ GeV/c;

$j_{i \text{ jet}} \leq 3$.

We do not apply a cut on $M(\mu^+ \mu^-)$ because of a singularity in the region $M(\mu^+ \mu^-) \rightarrow 0$ is regularized by massiveness of muon. Contributions of all subprocess to the total cross section is presented in the Table 1.

Table 1: Contributions to process $p p \rightarrow \mu^+ \mu^- + \text{jet}$ ($\sqrt{s_{pp}} = 5.5 \text{ TeV}$)

Subprocess:	Cross section (pb):
$u_h u_h \rightarrow \mu^+ \mu^- + g$	27.54
$d_h d_h \rightarrow \mu^+ \mu^- + g$	18.14
$u_h g \rightarrow \mu^+ \mu^- + u_h$	105.02
$d_h g \rightarrow \mu^+ \mu^- + d_h$	36.22
$u_h g \rightarrow \mu^+ \mu^- + u_h$	44.30
$d_h g \rightarrow \mu^+ \mu^- + d_h$	21.92
$bb \rightarrow \mu^+ \mu^- + g$	0.61
$bg \rightarrow \mu^+ \mu^- + b$	3.59
$bg \rightarrow \mu^+ \mu^- + b$	3.60
$qq \rightarrow \mu^+ \mu^- + q$	260.94

Note that the cross section for the process $p p \rightarrow \mu^+ \mu^- + \text{jet}$ was estimated in ref. [12] at RHIC and LHC energies taking into account the $q\bar{q}$ contribution only. Such approximation seems valid for RHIC, but for LHC the contribution from Z and γ - Z interference term are also significant.

Now we estimate the expected event rate for realistic geometrical acceptance and kinematic cuts. To be specific, the geometry of Compact Muon Solenoid (CMS) detector is considered [17, 18]: pseudo-rapidity coverage $|\eta| \leq 3$ for jets and $|\eta| \leq 2.4$ for muons. Extra cuts $P_T^{\mu^+} > 50 \text{ GeV}/c$ and $E_T^{\text{jet}} > 50 \text{ GeV}$ were applied. Then the corresponding pp cross section for $\mu^+ \mu^- + \text{jet}$ production is 16 pb , and Pb-Pb cross section is estimated as $16 \text{ pb} \times (207)^2 \approx 0.7 \text{ b}$. The corresponding event rate in a one month Pb-Pb run (assuming 15 days of data taking), $T = 1.3 \times 10^6 \text{ s}$, with designed luminosity $L = 10^{27} \text{ cm}^{-2} \text{ s}^{-1}$, is $N_{\text{ev}} = T \times \sigma_{\text{Pb-Pb}} \approx 1000$ in this case. Note that potential using also $e^+ e^- + \text{jet}$ channel could increase observed event rates by a factor ≈ 2 and requires further investigation.

To conclude this section, let us discuss the potential background sources. Semileptonic heavy quark decays and uncorrelated pion and kaon decays are expected to give main contributions to the dimuon spectra at LHC energies, $\approx 10^5$ events in a one month Pb-Pb run for CMS acceptance [8, 18]. However, the request of hard enough cut on muon pair transverse momentum, $P_T^{\mu^+} > 50 \text{ GeV}$, together with the additional trigger to have a hard jet with $E_T^{\text{jet}} > 50 \text{ GeV}$ in the opposite hemisphere, makes such background "contamination" negligible. Moreover, the experimental control on background extraction may be done by monitoring uncorrelated and correlated sources independently. The uncorrelated part can be subtracted using like-sign dimuon mass spectra, while the correlated part can be rejected using tracker information on the dimuon vertex position [8, 18].

3 Simulation of jet quenching at LHC

In order to generate the initial distributions of jets and $q\bar{q}$ pairs in nucleon-nucleon sub-collisions at $\sqrt{s} = 5.5$ TeV, we have used COMPHEP package for initial parton configuration setting and PYTHIA 6.2 [19] for subsequent jet fragmentation. After specifying initial partonic state, event-by-event Monte-Carlo simulation of rescattering and energy loss of partons in QGP is performed (for model details one can refer to the previous papers [20, 21]). The approach relies on an accumulative energy losses, when gluon radiation is associated with each scattering in expanding medium together including the interference effect by the modified radiation spectrum dE/dl as a function of decreasing temperature T . The basic kinetic integral equation for the energy loss E as a function of initial energy E_0 and path length L has the form

$$E(L; E_0) = \int_0^L dl \frac{dP(l)}{dl} \int_0^L dl' \frac{dE(l'; E_0)}{dl'}; \quad \frac{dP(l)}{dl} = \frac{1}{\lambda(l)} \exp(-l/\lambda(l)); \quad (1)$$

where l is the current transverse coordinate of a parton, dP/dl is the scattering probability density, dE/dl is the energy loss per unit length, $\lambda = 1/\sigma n$ is in-medium mean free path, n/T^3 is the medium density at the temperature T , σ is the integral cross section of parton interaction in the medium. Such numerical simulation of free path of a hard jet in QGP allows any kinematic characteristic distributions of jets in final state to be obtained.

The collisional energy loss due to elastic scattering with high-momentum transfer have been originally estimated by Bjorken in [22], and recalculated later in [23] taking also into account the loss with low-momentum transfer dominated by the interactions with plasma collective modes. Since latter process contributes to the total collisional loss without the large factor $\ln(E/m_D)$ (m_D is the Debye screening mass) in comparison with high-momentum scattering and it can be effectively "absorbed" by the redefinition of minimal momentum transfer t_{\min}^2 under the numerical estimates, we used the collisional part with high-momentum transfer only [21],

$$\frac{dE^{\text{coll}}}{dl} = \frac{1}{4T} \int_{t_{\min}^2}^{3T^2 E^2} dt \frac{d}{dt} t; \quad (2)$$

and the dominant contribution to the differential cross section

$$\frac{d}{dt} = C \frac{2}{t^2} \alpha_s^2(t); \quad \sigma_s = \frac{12}{(33 - 2N_f) \ln(t/Q_{CD}^2)} \quad (3)$$

for scattering of a parton with energy E on the "thermal" partons with energy (or effective mass) $m_0 = 3T \ll E$. Here $C = 9/4; 1/4; 9$ for gg, gq and qq scatterings respectively, α_s is the QCD running coupling constant for N_f active quark flavors, and Q_{CD} is the QCD scale parameter

which is of the order of the critical temperature, $T_c \approx 200 \text{ MeV}$. The integrated cross section is regularized by the Debye screening mass squared $\mu_D^2(T) \approx 4\pi s T^2 (1 + N_f/6)$.

There are several calculations of the inclusive energy distribution of medium-induced gluon radiation from Feynman multiple scattering diagrams. The relation between these approaches and their main parameters were discussed in details in the recent writeup of the working group "Jet Physics" for the CERN Yellow Report [7]. We restrict to ourselves here by using BDMSS formalism [24]. In the BDMSS framework the strength of multiple scattering is characterized by the transport coefficient $\hat{q} = \frac{2}{D} = \frac{1}{\lambda_g}$ (λ_g is the gluon mean free path), which is related to the elastic scattering cross section (3). In our simulations this strength in fact is regulated mainly by the initial temperature T_0 . Then the energy spectrum of coherent medium-induced gluon radiation and the corresponding dominated part of radiative energy loss has the form [24]:

$$\frac{dE^{\text{rad}}}{dL} = \frac{2s(\frac{2}{D})C_R}{L} \int_{\lambda_{\text{min}}}^E d\lambda \left(1 - y + \frac{y^2}{2} \ln \left[\frac{2E}{\lambda(1-y)} \right] \right); \quad (4)$$

$$\lambda_{\text{min}} = \lambda \left(1 - y + \frac{C_R}{3} y^2 \ln \frac{16}{3}\right) \quad \text{with} \quad \lambda = \frac{2}{D} \frac{g}{(1-y)}; \quad (5)$$

where $\lambda = L/(2\lambda_g)$, $y = E/\lambda$ is the fraction of the hard parton energy carried by the radiated gluon, and $C_R = 4/3$ is the quark color factor. A similar expression for the gluon jet can be obtained by substituting $C_R = 3$ and a proper change of the factor in the square bracket in (4), see ref. [24]. The integral (4) is carried out over all energies from $\lambda_{\text{min}} = E_{\text{LPM}} = \frac{2}{D} \lambda_g$, the minimal radiated gluon energy in the coherent LPM regime, up to initial jet energy E .

The medium was treated as a boost-invariant longitudinally expanding quark-gluon fluid, and partons as being produced on a hyper-surface of equal proper times [25]. In order to simplify numerical calculations (and not to introduce new parameters) we omit the transverse expansion and viscosity of the fluid using the well-known scaling Bjorken's solution [25] for temperature and density of QGP at $T > T_c \approx 200 \text{ MeV}$:

$$T(\tau) \approx T_0 \tau^{-1/3}; \quad T(\tau) \approx T_0 \tau^{-1/3}; \quad (\tau) = \tau_0: \quad (6)$$

Let us remark that the influence of the transverse flow, as well as of the mixed phase at $T = T_c$, on the intensity of jet rescattering (which is a strongly increasing function of T) is inessential for high initial temperatures $T_0 \gg T_c$ [20, 21]. On the contrary, the presence of viscosity slows down the cooling rate, which leads to a jet parton spending more time in the hottest regions of the medium. As a result the rescattering intensity goes up, i.e., in fact an effective temperature of the medium gets lifted as compared with the perfect QGP [20, 21]. We also do not take into account here the probability of jet rescattering in nuclear matter, because the intensity of this process and corresponding contribution to total energy loss are negligible due to much

smaller energy density in a "cold" nuclei. For certainty we used the initial conditions for the gluon-dominated plasma formation expected for central Pb-Pb collisions at LHC [26]:

$$\rho_0 \approx 0.1 \text{ fm}^{-3}; \quad T_0 \approx 1 \text{ GeV}; \quad g \approx 1.95T^3 :$$

For non-central collisions we suggest the proportionality of the initial energy density ρ_0 to the ratio of nuclear overlap function and effective transverse area of nuclear overlapping [21].

In each event the distribution of jet production vertex at the given impact parameter b of AA collision is generated according to the distribution [21]

$$\frac{dN^{\text{jet}}}{d^2r} (b) = \frac{T_A(r_1)T_A(r_2)}{\int_0^{R_A} \int_0^{R_A} r dr T_A(r_1)T_A(r_2)}; \quad (7)$$

where $r_{1,2}(b;r)$ are the distances between the nucleus centers and the jet production vertex $V(r \cos \phi; r \sin \phi)$; $r_{\text{max}}(b)$ is the maximum possible transverse distance r from the nuclear collision axis to the V ; R_A is the radius of the nucleus A ; $T_A(r_{1,2})$ is the nuclear thickness function (see ref. [21] for detailed nuclear geometry explanations). After that, in every i -th scattering of the co-moving particle (with the same longitudinal rapidity) a fast parton loses energy in the collisions and radiatively, $e_i = t_i = (2m_0) + \epsilon_i$, where t_i and ϵ_i are simulated according to eqs. (2) and (4) respectively. Thus in each event the energy of an initial parton decreases by value $E(r) = \prod_i e_i$.

In the frame of this model and using above QGP parameters we evaluate the mean energy loss of quark of $E_T = 50 \text{ GeV}$ in minimum bias Pb-Pb collisions, $\langle E_T^q \rangle \approx 25 \text{ GeV}$. In order to analyze the sensitivity of di-jet correlations to the absolute value of partonic energy loss, we also performed the same calculations for the reduced initial temperature, $T_0 = 0.7 \text{ GeV}$, which results in decreasing average energy loss by a factor $(1=0.7)^3 \approx 0.34$.

The distribution over a difference between P_T^+ , transverse momentum of $+$ pair, and E_T^{jet} , observed transverse energy of jet, depends crucially on a fraction of the partonic energy loss falling outside the jet cone. There are some discussions on an angular spectrum of in-medium radiated gluons in the literature [20, 24, 27, 28, 29]. In fact, since the coherent Landau-Pomeranchuk-Migdal radiation induces a strong dependence of the radiative energy loss of a jet on the angular cone size, it will soften particle energy distributions inside the jet, increase the multiplicity of secondary particles, and to a lesser degree, affects the total jet energy. On the other hand, the energy loss in the collisions turns out to be practically independent of the jet cone size and causes the loss of the total jet energy, because the bulk of "them all" particles knocked out of the dense matter by the elastic scatterings flies away in almost transverse direction relatively to the jet axis [20]. Thus, although the radiative

energy loss of the energetic parton dominates over the loss in the collisions by up to an order of magnitude, the relative contribution of the latter jet energy loss grows with increasing the jet cone size due to essentially different angular structure of loss for two mechanisms [20]. Moreover, the total energy loss of a jet will be sensitive to the experimental capabilities to detect low p_T particles (products of soft gluon fragmentation: thresholds for giving signal in calorimeters, influence of strong magnetic field, etc. [18]).

Since the full treatment of angular spectrum of emitted gluons is rather sophisticated and model-dependent [20, 24, 27, 28, 29], we considered two simple parameterizations of distribution of in-medium radiated gluons over emission angle θ . The "small-angular" radiation spectrum was parameterized in the form

$$\frac{dN^g}{d\theta} \sim \exp\left(-\frac{\theta}{\theta_0}\right)^2; \quad (8)$$

where $\theta_0 \approx 5^\circ$ is the typical angle of coherent gluon radiation estimated in work [20]. The "broad-angular" spectrum has the form

$$\frac{dN^g}{d\theta} \sim \frac{1}{\theta}; \quad (9)$$

We believe that the such simplified treatment here is enough to demonstrate the sensitivity of p_T -balance in $^+ +$ jet production to the medium-induced partonic energy loss.

4 Numerical results and discussion

To be specific, the jet energy is defined here as the total transverse energy of final particles collected around the direction of a leading particle inside the cone $R = \sqrt{\frac{\Delta\eta^2 + \Delta\phi^2}{2}} = 0.5$, where $\Delta\eta$ and $\Delta\phi$ are the pseudorapidity and the azimuthal angle respectively. Fig.2 shows the distribution over p_T^+ E_T^{jet} for the cases without and with medium-induced energy loss obtained in the framework of our model in minimum-bias Pb-Pb collisions, two parameterizations of distribution on gluon emission angles (8) and (9) being used. The same geometrical acceptance and kinematic cuts as in Sect.2 were applied: $j^{\text{jet}} \leq 3$, $j \leq 2.4$, $p_T > 5 \text{ GeV}/c$, $p_T^+; E_T^{\text{jet}} > 50 \text{ GeV}$. Although $p_T^+ E_T^{\text{jet}}$ -distribution is already smeared in pp case, mainly due to the initial state gluon radiation, the mean value $\langle p_T^+ E_T^{\text{jet}} \rangle$, as well as the maximum of the distribution are close to 0. The partonic energy loss in heavy ion collisions results in the visible asymmetry of this distribution, its significant smearing and shifting mean and maximum values. The effect is more pronounced for the "broad-angular" radiation, because the contribution of the "out-of-cone" partonic energy loss is larger as compared with the "small-angular" radiation case. Note that for jet of cone $R = 0.5$ the contribution to jet energy loss from collisional part becomes comparable with the contribution from "small-angular"

gluon radiation. The latter does not disappear totally mostly due to the fact that not only leading (parent) parton, but all partons of a jet pass through the dense medium and emit gluons under the angles relatively to their proper directions, which in general may not coincide with the jet axis (determined by the direction of a leading particle) and sometimes be even at the jet periphery. Thus in the case of "isotropic" radiation, di-jet correlation will be significantly sensitive to the collisional part of the loss.

However in a real experimental situation the jet observables will be sensitive to the accuracy of jet energy reconstruction in high multiplicity environment. There are the two terms determining this accuracy: systematic jet energy loss and jet energy resolution (due to calorimeter and jet peculiarities, influence of magnetic field, etc.). Short measure of jet energy will be well-controlled systematic error which has the similar values for heavy ion and for pp collisions, and it can be taken into account using the standard calibration procedure [30]. On the other hand, the finite jet energy resolution will result in additional smearing $P_T^+ \rightarrow E_T^{\text{jet}}$ distribution without shifting mean and maximum values. In order to illustrate the sensitivity of such observables to experimental jet energy resolution δ_{E_T} , we set for definiteness the simple parameterization, $\delta_{E_T} = 1.5 \frac{P}{E_T} \text{ GeV}$, which is close to one obtained with window-type jet finding algorithm for central Pb-Pb collisions at CMS [7]. Fig.3 shows the same distribution as Fig.2, but initial jet energy was smeared in each event by value δ_{E_T} . Due to additional smearing the initial distribution, the effect of jet quenching on shifting mean and maximum values becomes less visible and rather marginal for moderate partonic energy loss.

Since jet observables are affected by a number of theoretical (in particular, sensitivity to the angular spectrum of medium-induced radiation and to the collisional part of energy loss) and methodical (finite jet energy resolution) uncertainties, complementary leading particle measurements are potentially important, such as p_T -balance between muon pairs and a leading particle in a jet. Fig.4 presents the distribution over variable $P_T^+ \rightarrow 5 E_T^{\text{leader}}$ (under the same conditions as for Fig.2), where E_T^{leader} is the transverse energy of a leading particle (i.e. particle with maximum E_T) in a jet. The choice of a factor of 5 denotes only the fact that the most probable value of a fraction of jet energy carried by leading particles is 0.2 in our case. This distribution is originally more smeared and asymmetric than the distribution over $P_T^+ \rightarrow E_T^{\text{jet}}$. However additional smearing and shifting mean and maximum values due to partonic energy loss can be also clearly seen even for relatively small loss, $\langle E_T^{\text{gluon}} \rangle = 8 \text{ GeV}$ at $T_0 = 0.7$ ($\rho = 0$) GeV. Moreover, the observed p_T -balance between μ^+ pair and a leading particle in a jet is directly related to the absolute value of partonic energy loss and almost insensitive to the form of the angular spectrum of emitted gluons. The small difference for various angular distributions is just due to the moderate distinction of event samples which

were triggered by having a jet with $E_T^{\text{jet}} > 50 \text{ GeV}$. Since fixing the minimum threshold for jet detection is sensitive to the total jet energy (and consequently to the angular dependence of energy loss), the small influence of the latter on diuon-leader correlation appears. We also become convinced that taking into account the jet energy smearing δE_T almost does not have influence on diuon-leader correlation (see Fig. 5).

5 Conclusions

The channel with diuon tagged jet production in ultrarelativistic heavy ion collisions was analyzed. The cross section of this process and corresponding event rates at LHC energies were evaluated with COMBHEP Monte-Carlo generator taking into account full γZ interference pattern. The reasonable statistics, 1000 events per month of LHC run with lead beams, can be expected for realistic geometrical acceptance and kinematic cuts.

The correlations between q^+ pair and jet, as well as between q^+ pair and a leading particle in a jet, were first numerically studied for heavy ion collisions. The medium-induced partonic energy loss can result in significant smearing the distribution on difference between the transverse momentum of q^+ pair and the jet transverse energy, and shifting mean and maximum values of the distribution. This effect will be sensitive to the fraction of partonic energy loss (dependent on the form of the angular spectrum of in-medium radiated gluons) falling outside the jet cone. However the finite experimental jet energy resolution can result in additional smearing diuon-jet correlation, which can make difficult observation of P_T -in balance especially for moderate partonic energy loss.

Since jet observables are affected by a number of theoretical and methodical uncertainties, complementary leading particle measurements will be useful and even preferable. P_T -in balance between q^+ pair and a leading particle in a jet is quite visible even for moderate loss, directly related to the absolute value of partonic energy loss, almost insensitive to the angular spectrum of emitted gluons and to experimental jet energy resolution.

Finally, the study of $q^+ + \text{jet}$ and q^+ -leading-particle correlations is important for extracting the information about medium-induced partonic energy loss and properties of superdense QCD matter to be created in heavy ion collisions at the LHC.

Acknowledgments. Discussions with E.E. Boos and L.I. Sarycheva are gratefully acknowledged. This work is supported by grants N 04-02-16333 and N 04-02-17448 of Russian Foundation for Basic Research, and the grant of the Program "Universities of Russia" UR.02.03.028.

References

- [1] R. Baier, D. Schi, and B.G. Zakharov, *Annual Rev. Nucl. Part. Sci.* 50 (2000) 37.
- [2] STAR Collab., C Adler et al., *Nucl. Phys. A* 698 (2002) 64; *Phys. Rev. Lett.* 89 (2002) 202301.
- [3] PHENIX Collab., K Adcox et al., *Nucl. Phys. A* 698 (2002) 511; *Phys. Rev. Lett.* 88 (2002) 022301.
- [4] PHOBOS Collab., B.B. Back et al., *Nucl. Phys. A* 698 (2002) 655.
- [5] BRAHMS Collab., I.G. Bearden et al., *Nucl. Phys. A* 698 (2002) 29.
- [6] X.-N. Wang, *Phys. Lett. B* 579 (2004) 299.
- [7] A. Accardi et al., writeup of the working group "Jet Physics" for the CERN Yellow Report on "Hard Probes in Heavy Ion Collisions at the LHC", hep-ph/0310274.
- [8] M. Bedjidian et al., writeup of the working group "Heavy Flavour Physics" for the CERN Yellow Report on "Hard Probes in Heavy Ion Collisions at the LHC", hep-ph/0311048.
- [9] R. Arleo et al., writeup of the working group "Photon Physics" for the CERN Yellow Report on "Hard Probes in Heavy Ion Collisions at the LHC", hep-ph/0311131.
- [10] X.-N. Wang, Z. Huang, and I. Sarcevic, *Phys. Rev. Lett.* 231 (1996) 77; X.-N. Wang and Z. Huang, *Phys. Rev. C* 55 (1997) 3047.
- [11] V. Kartvelishvili, R. Kvatadze, and R. Shanidze, *Phys. Lett. B* 356 (1995) 589.
- [12] D.K. Srivastava, C. Gale, and T.C. Awes, *Phys. Rev. C* 67 (2003) 054904.
- [13] O.L. Kodolova et al., CERN CMS Note 1998/063; O.L. Kodolova, I.P. Lokhtin, and A. Nikitenko, hep-ph/0212052.
- [14] COMPHEP Collab., E. Boos et al., hep-ph/0403113.
- [15] E.E. Boos, V.A. Ilyin, and A.N. Skachkova, *JHEP* 0005 (2000) 052.
- [16] CTEQ Collab., H.L. Lai et al., *Eur. Phys. J. C* 12 (2000) 375.
- [17] CMS Collab., Technical Proposal, CERN/LHCC 94-38.
- [18] G. Baur et al., "Heavy Ion Physics Programme in CMS", CERN CMS Note 2000/060.

- [19] T. Sjöstrand, *Comp. Phys. Comm.* 135 (2001) 238.
- [20] I.P. Lokhtin and A.M. Snigirev, *Phys. Lett. B* 440 (1998) 163.
- [21] I.P. Lokhtin and A.M. Snigirev, *Eur. Phys. J. C* 16 (2000) 527.
- [22] J.D. Bjorken, Fermilab publication Pub-82/29-THY (1982).
- [23] S. Mrowczynski, *Phys. Lett. B* 269 (1991) 383; M.H. Thomas, *Phys. Lett. B* 273 (1991) 128.
- [24] R. Baier, Yu.L. Dokshitzer, A.H. Mueller, and D. Schi, *Phys. Rev. C* 60 (1999) 064902; *Phys. Rev. C* 64 (2001) 057902.
- [25] J.D. Bjorken, *Phys. Rev. D* 27 (1983) 140.
- [26] K.J. Eskola, K. Kajantie, and K. Tuominen, *Phys. Lett. B* 497 (2001) 39; K.J. Eskola, P.V. Ruuskanen, S.S. Rasanen, and K. Tuominen, *Nucl. Phys. A* 696 (2001) 715.
- [27] B.G. Zakharov, *JETP Lett.* 70 (1999) 176.
- [28] U.A. Wiedemann and M. Gyulassy, *Nucl. Phys. B* 560 (1999) 345; U.A. Wiedemann, *Nucl. Phys. B* 588 (2000) 303; *Nucl. Phys. A* 690 (2001) 731.
- [29] M. Gyulassy, P. Levai, and I. Vitev, *Nucl. Phys. B* 571 (2000) 197; *Phys. Rev. Lett.* 85 (2000) 5535; *Nucl. Phys. B* 594 (2001) 371.
- [30] O. Kodolova, S. Kunori, A. Oulianov, and I. Vardanian, CERN CM S Note 2002/023

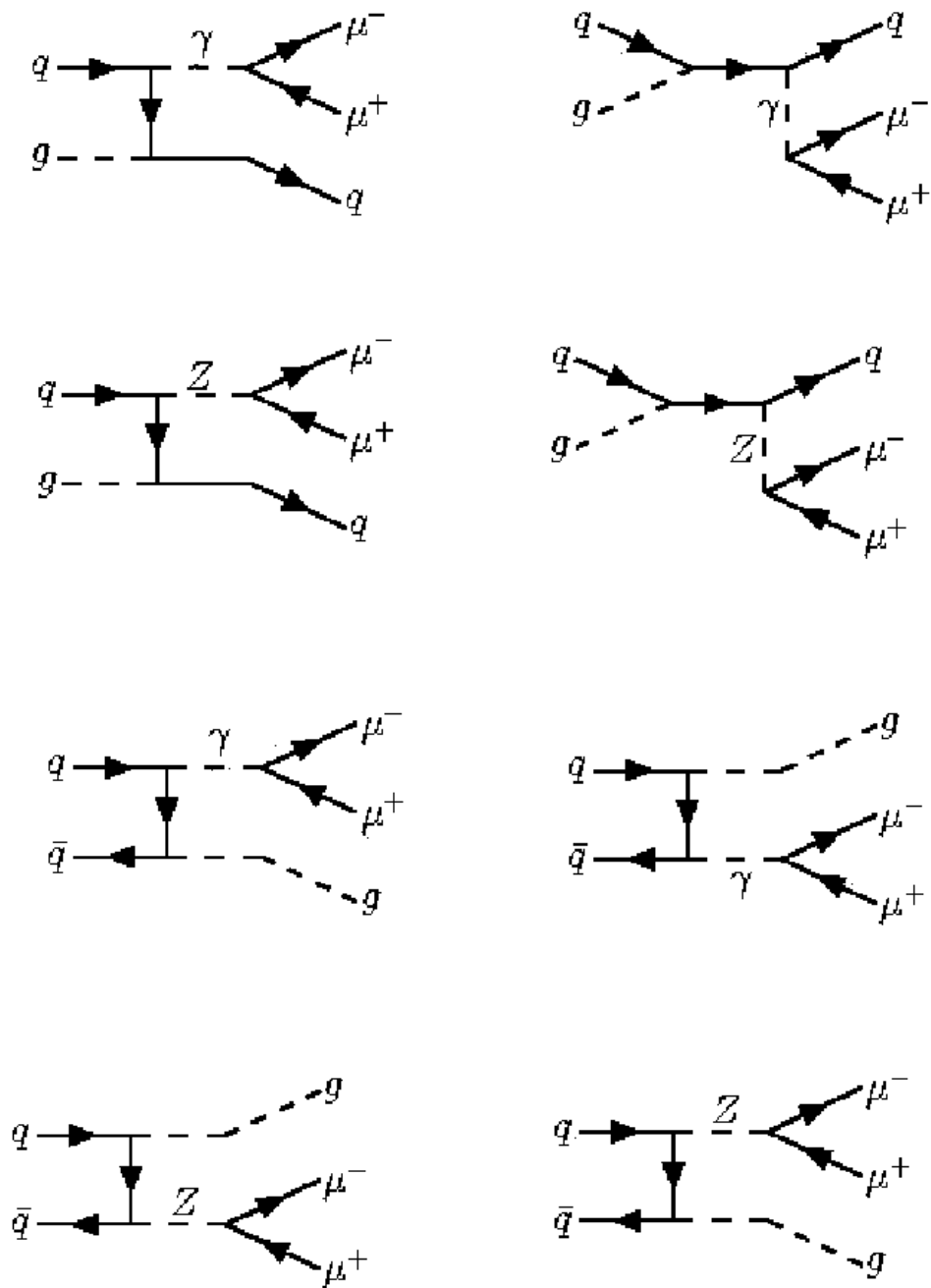


Figure 1: Feynman diagrams for processes $qg \rightarrow q + \mu^+ \mu^-$ and $q\bar{q} \rightarrow g + \mu^+ \mu^-$ in the leading order approximation of SM.

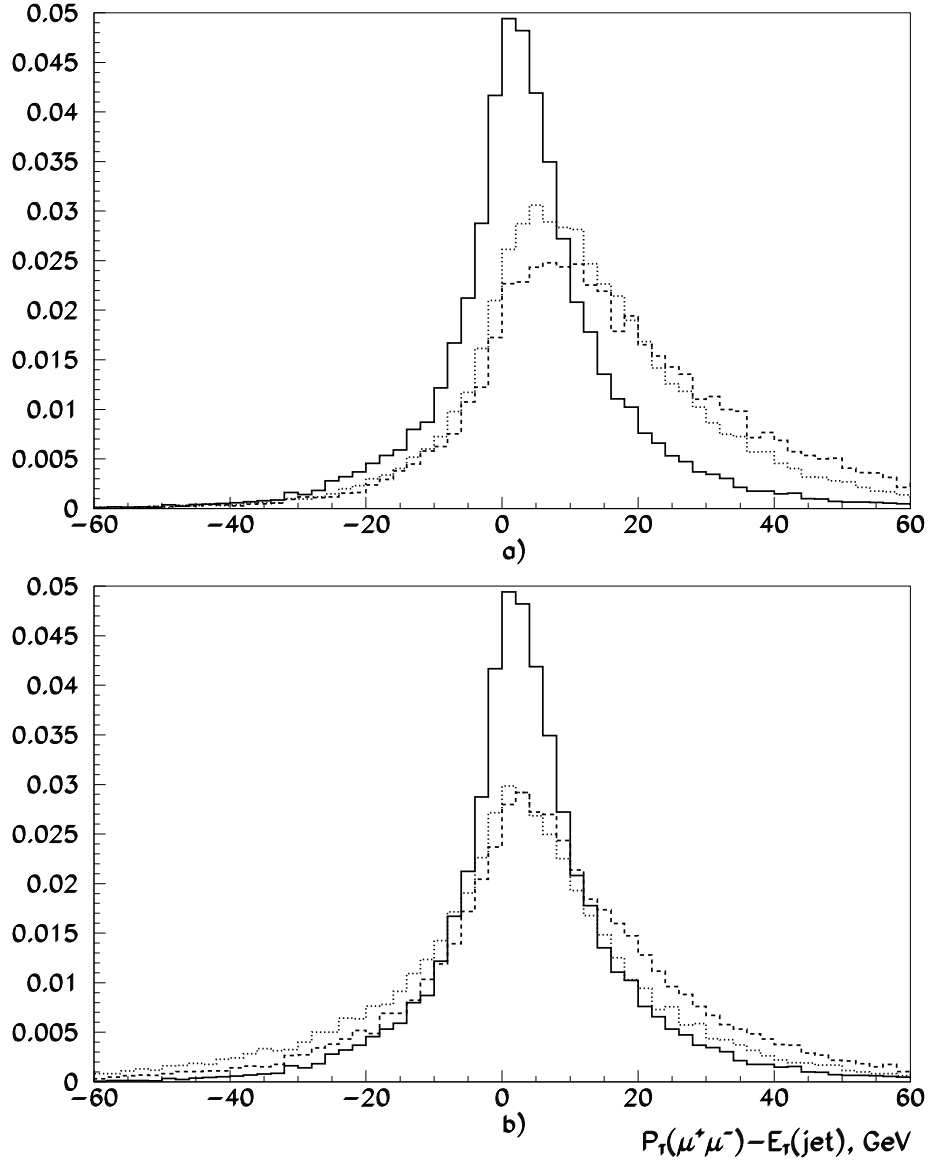


Figure 2: The distribution over difference between the transverse momentum of $\mu^+ \mu^-$ pair, P_T^+ , and the jet transverse energy, E_T^{jet} , without (solid histogram) and with medium-induced partonic energy loss for the "all-angular" (8) (dotted histogram) and the "broad-angular" (9) (dashed histogram) parameterizations of an fitted gluon spectrum in minimum-bias Pb-Pb collisions. Applied kinematical cuts are described in the text. Initial QGP temperature $T_0 = 1$ (a) $T_0 = 0.7$ (b) GeV.

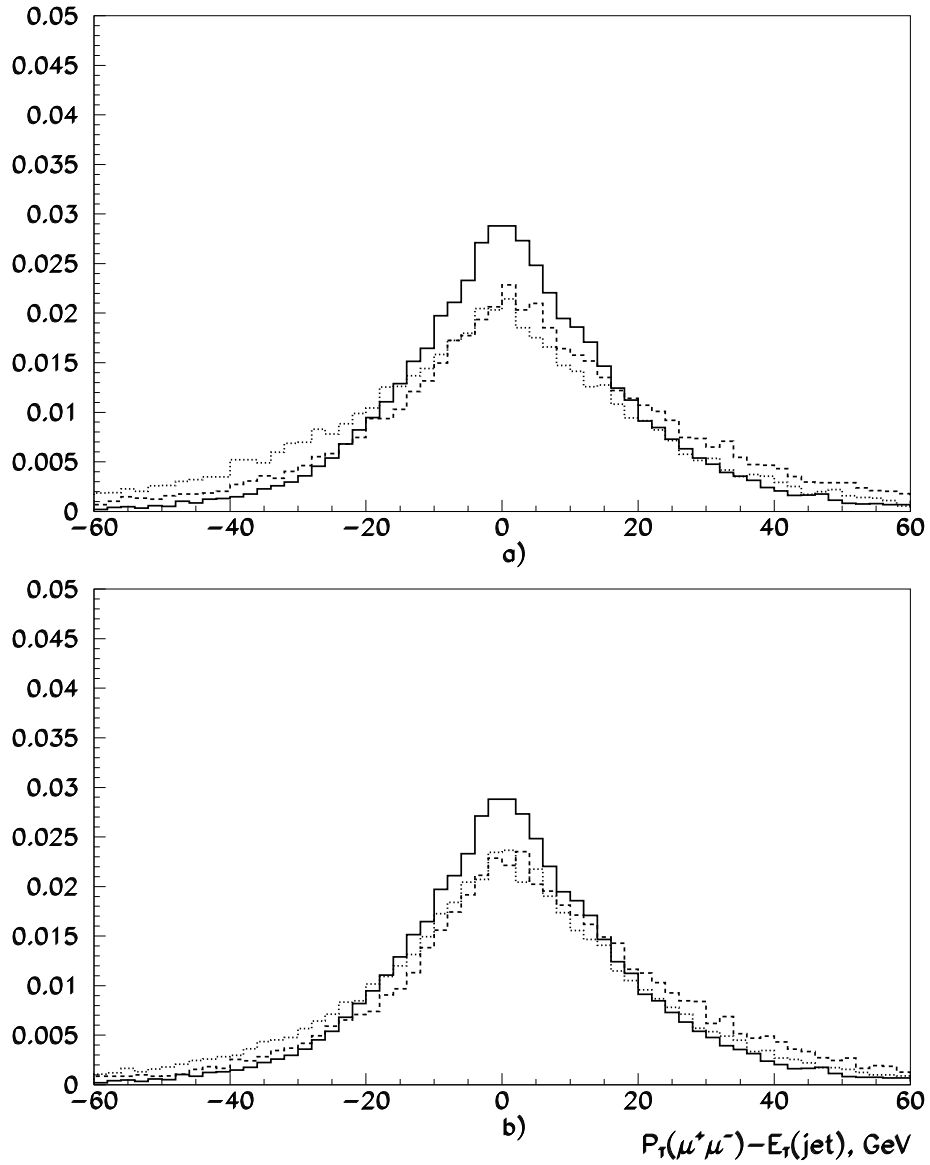


Figure 3: The same as in Fig. 2, but including jet energy "smearing", $E_T = 1.5 \frac{p}{E_T} \text{ GeV}$.

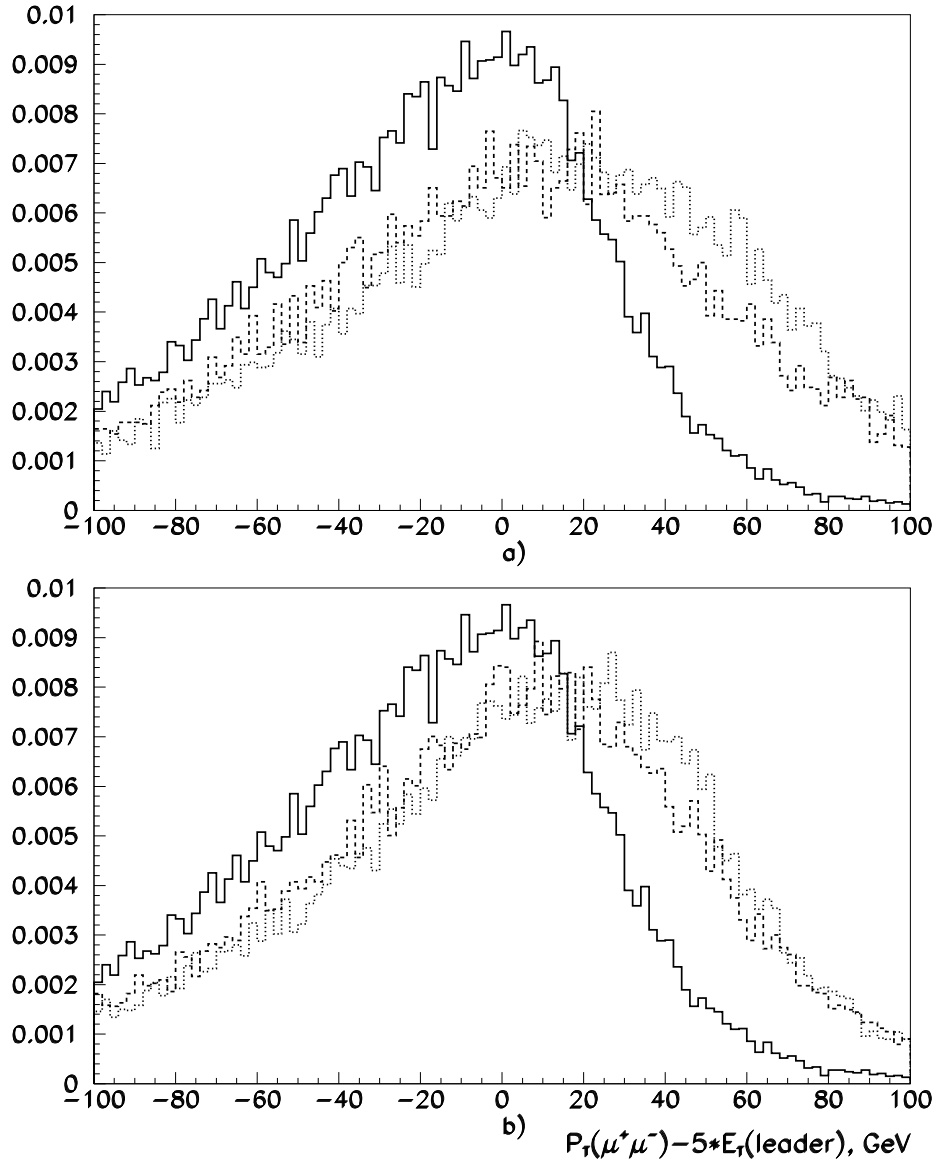


Figure 4: The distribution over difference between the transverse momentum of $\mu^+\mu^-$ pair, P_T^+ , and five times transverse energy of a leading particle in a jet, $5 E_T^{\text{leader}}$. The other conditions are the same as for fig. 2.

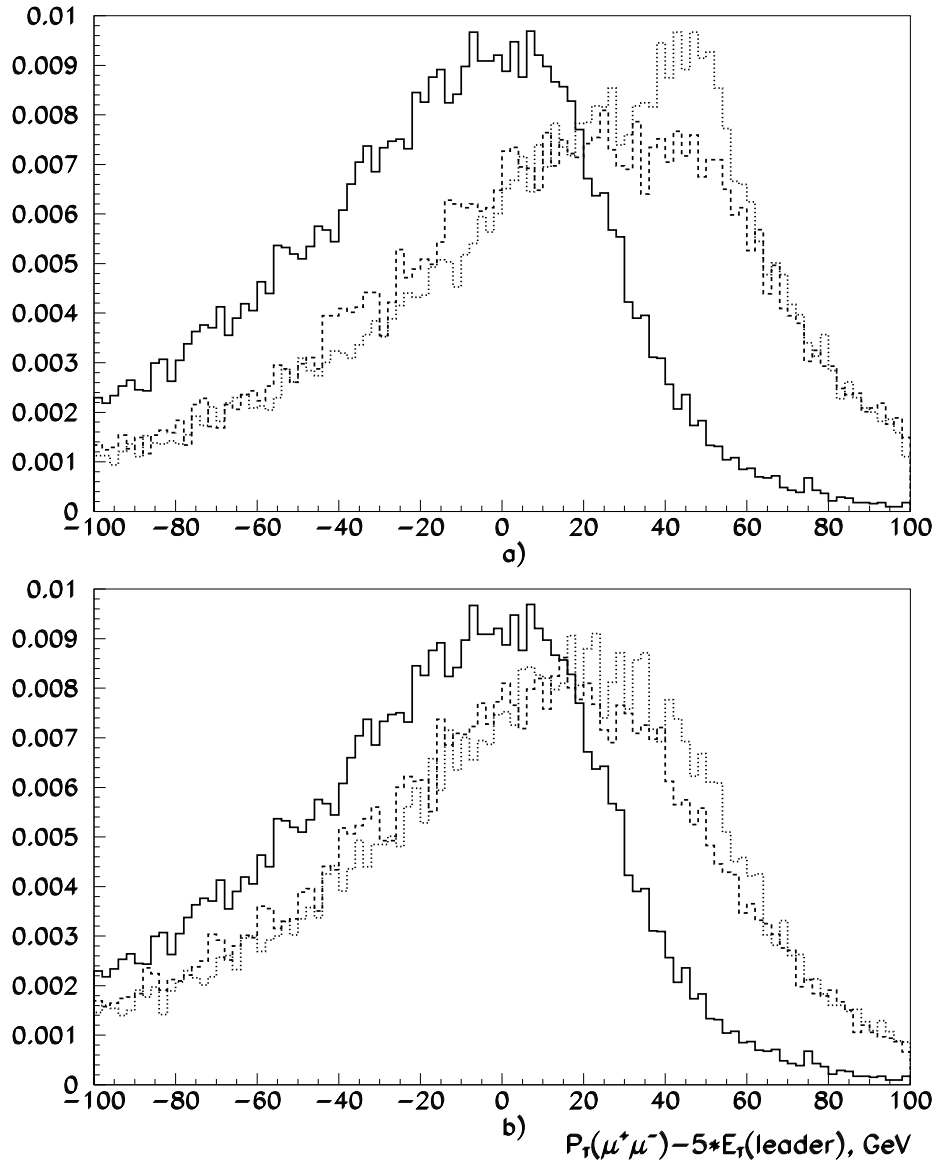


Figure 5: The same as in Fig. 4, but including jet energy "earing", $\sqrt{s} = 1.5 \sqrt{E_T} \text{ GeV}$.